



Discovery of potent selective bioavailable phosphodiesterase 2 (PDE2) inhibitors active in an osteoarthritis pain model. Part II: Optimization studies and demonstration of in vivo efficacy



Mark S. Plummer^{a,*}, Joseph Cornicelli^b, Howard Roark^a, Donald J. Skalitzky^a, Charles J. Stankovic^d, Susan Bove^b, Jayvardhan Pandit^c, Annise Goodman^a, James Hicks^a, Aurash Shahripour^a, David Beidler^b, Xiao Kang Lu^b, Brian Sanchez^b, Christopher Whitehead^a, Ron Sarver^e, Timothy Braden^b, Richard Gowan^b, Xi Qiang Shen^b, Katherine Welch^b, Adam Ogden^d, Nalini Sadagopan^d, Heidi Baum^d, Howard Miller^d, Craig Banotai^e, Cindy Spessard^e, Sandra Lightle^e

^a Department of Chemistry, Pfizer Global Research and Development, Ann Arbor, MI 48105, USA

^b Inflammation Pharmacology, Pfizer Global Research and Development, Ann Arbor, MI 48105, USA

^c Discovery Technology, Pfizer Global Research and Development, Groton, CT 06340, USA

^d Pharmacodynamics and Drug Metabolism, Pfizer Global Research and Development, Ann Arbor, MI 48105, USA

^e Discovery Technology, Pfizer Global Research and Development, Ann Arbor, MI 48105, USA

ARTICLE INFO

Article history:

Available online 29 March 2013

Keywords:

Phosphodiesterase 2 (PDE2) inhibitors
Structure based drug design
Osteoarthritis (OA) pain

ABSTRACT

Selective phosphodiesterase 2 (PDE2) inhibitors are shown to have efficacy in a rat model of osteoarthritis (OA) pain. We identified potent, selective PDE2 inhibitors by optimizing residual PDE2 activity in a series of phosphodiesterase 4 (PDE4) inhibitors, while minimizing PDE4 inhibitory activity. These newly designed PDE2 inhibitors bind to the PDE2 enzyme in a cGMP-like binding mode orthogonal to the cAMP-like binding mode found in PDE4. Extensive structure activity relationship studies ultimately led to identification of pyrazolodiazepinone, **22**, which was >1000-fold selective for PDE2 over recombinant, full length PDEs 1B, 3A, 3B, 4A, 4B, 4C, 7A, 7B, 8A, 8B, 9, 10 and 11. Compound **22** also retained excellent PDE2 selectivity (241-fold to 419-fold) over the remaining recombinant, full length PDEs, 1A, 4D, 5, and 6. Compound **22** exhibited good pharmacokinetic properties and excellent oral bioavailability ($F = 78\%$, rat). In an in vivo rat model of OA pain, compound **22** had significant analgesic activity 1 and 3 h after a single, 10 mg/kg, subcutaneous dose.

© 2013 Elsevier Ltd. All rights reserved.

In our previous letter we reported that pyrazolodiazepinone inhibitors selective for PDE2 were identified from structure activity studies. We were interested in pursuing peripherally restricted PDE2 inhibitors as a potential treatment for OA pain. The impetus for our interest originated in an indications discovery effort to identify novel analgesic mechanisms, where we observed antinociceptive activity when employing selective PDE2 inhibitors. The role of PDE2 in the production and modulation of pain is inferred from a number of observations including that PDE2 is highly expressed in the brain, spinal cord, dorsal root ganglia (DRG) as well as several non-pain related tissues.¹ Additionally the non-hydrolyzable cGMP analog, 8-bromo-cGMP, has been shown to reduce nociceptive behavior in rats at low doses in formalin-induced inflammatory pain.² Selective inhibition of PDE2 elevates cGMP in cells or subcellular compartments where it is located.³ Collectively this suggests

raising cGMP levels through PDE2 inhibition may provide a potential treatment for OA pain. We were particularly interested in peripheral PDE2 inhibition in the DRG as a mechanism to avoid potential but unknown side effects of a centrally acting agent.

The design premise was that diazepinones could be made PDE2 selective by virtue of a cGMP-like binding mode to an active site glutamine, Gln859 in PDE2. This cGMP-like binding mode is orthogonal to that of the diazepinone cAMP-like binding mode in PDE4 due to a glutamine switch.⁴ The presence of the cGMP-like binding mode was confirmed by a crystal structure of a PDE2 selective inhibitor **1** bound to the active site of the PDE2 catalytic domain, PBP ID 4JIB (Fig. 1).

We identified diazepinone PDE2 inhibitors with submicromolar potency and modest selectivity (33-fold) versus PDE4 as described in the previous paper. However, these inhibitors suffered from poor microsomal stability. At this point we shifted our strategy, abandoning biaryl substituted imidazoles, as found in **1**, for a more metabolically stable 3,4-dimethoxyphenyl group and worked to

* Corresponding author.

E-mail address: marksplummer@gmail.com (M.S. Plummer).

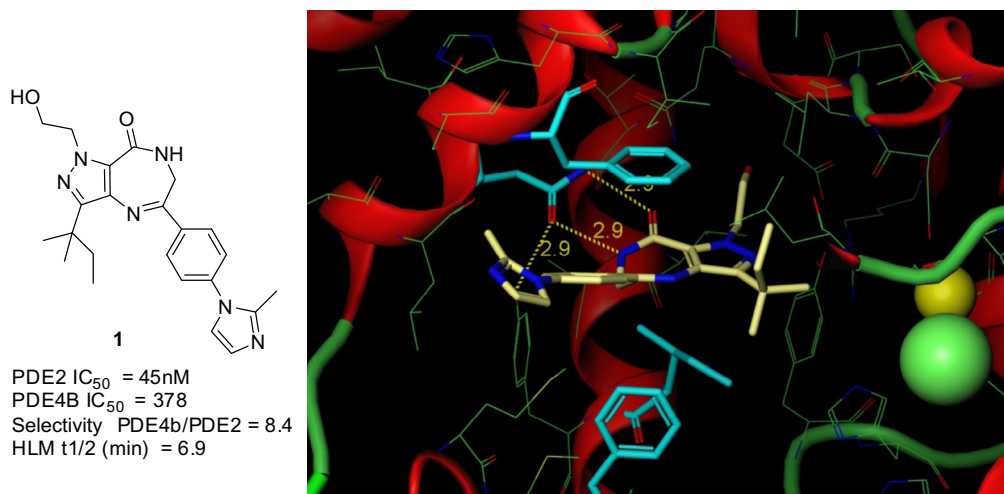


Figure 1. The PDE2 selective inhibitor, **1**, crystallized with the PDE2 catalytic domain, PBP ID 4JIB.

exploit the cGMP-like orthogonal binding mode to produce nanomolar potent PDE2 inhibitors with greater than 100 fold selectivity versus other PDEs.

The X-ray structure of **1** reveals several points to differentiate PDE2 inhibition from PDE4 inhibition. Firstly the inhibitor **1** binds in an orthogonal manner to PDE2 wherein the hydroxyethyl side chain points to the interior of the binding pocket, with a hydrogen bond interaction between the hydroxyl group of the inhibitor and Gln812. In PDE4, the residue corresponding to Gln812 is a proline which cannot form such a hydrogen bond. This additional interaction and the size of the surrounding pocket are points of differentiation. The crystal structure also reveals several hydrophobic residues adjacent to the phenyl group of the phenylimidazole moiety at the entrance to the binding pocket, suggesting an additional area to further optimize PDE2 inhibition and selectivity.

The hydrophobic area adjacent to the phenyl ring was especially attractive as the metabolically more stable 3,4-dimethoxyphenyl group led directly to design of 3-aryl-4-methoxyphenyl moieties, enabling the exploration of the adjacent hydrophobic region. This phenyl substitution improved selective inhibition of PDE2 over PDE4 as seen in **2** and **3** when compared with **1** (Table 1). These compounds were conveniently prepared by late-stage Suzuki coupling of the corresponding 3-bromo-4-methoxyphenyldiazepinone (**V**). The general synthetic route to the key intermediate (**V**) was described in our previous paper. Synthesis of the required amino ketone was accomplished by reaction of 3-bromo-4-methoxychloroacetophenone with sodium biformylamide followed by acid hydrolysis to give 3-bromo-4-methoxyphenylaminoketone hydrochloride **III** (Scheme 1).⁵

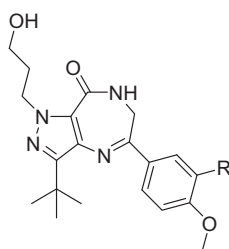
To explore interactions with Gln812 more fully, we targeted hydroxypropyl substituted pyrazoles to establish the degree of selectivity for PDE2 versus PDE4, because this functionality was previously found to impart superior PDE2/PDE4 selectivity and had greater metabolic stability than the corresponding hydroxyethyl analogs. We postulated that improved selectivity would directly translate to the more potent hydroxyethyl pyrazole series. Recall, the aryl group of the 3-aryl-4-methoxyphenyl substituent was designed to interact with the rather hydrophobic exit from the PDE2 catalytic active site, suggesting that hydrophobic biaryl moieties would result in increased PDE2 inhibition and selectivity. Surprisingly, the most hydrophobic residues, as in **2–5**, had the poorest PDE2 activity in the series (Table 1). Addition of slightly more polar functionality gave the 2,5-dimethoxy analog, **6**, resulting in a threefold increase in PDE2 inhibition and 176-fold selectivity

over PDE4. The 2,4-dimethoxy analog **7** provided even greater PDE2 inhibition (PDE2 IC₅₀ = 14 nM) and 200-fold selectivity. The requirement of a polar hydrogen bond acceptor is illustrated by the carboxyl functionality in **8** a potent PDE2 inhibitor with 675-fold selectivity. Indeed, a variety of hydrogen bond acceptor heterocyclic biaryl groups as in **9–12** provided potent PDE2 inhibition with greater than 100-fold selectivity over PDE4 (Table 1). These heterocyclic biaryl groups also provided a structural basis for the modification of physicochemical properties (Log*P*, Log*D*, and aqueous solubility) which yielded significantly improved human liver microsomal stability as compared to the more hydrophobic analogs.

The recently published PDE2A (215–900) crystal structure⁶ provides insight into the significant SAR observed with the distal aryl ring that extends out of the catalytic site. The structure shows that PDE2A exists as a dimer with the H-loops of the catalytic subunits packing against each other at the dimer interface, occluding the catalytic sites. The model predicts that cGMP binding to the GAF-B domain, facilitates movement of the H-loops, so that they no longer pack at the dimer interface allowing access to the catalytic site. We speculate that the distal aryl ring in our inhibitors may interact either with residues in the H-loop or some aspect of the catalytic domain in the adjacent strand of the dimer.

Four of the most PDE2-selective analogs, **7** and **10–12**, were synthesized with the more potent but potentially less selective hydroxyethyl substituted pyrazole moiety to provide **13–16** (Table 2). As expected, three of the hydroxyethyl compounds had significantly improved PDE2 potency compared with the hydroxypropyl series, (**7** vs **15**; **10** vs **13**; **11** vs **14**). The remaining matched pair (**12**, **16**) had equivalent potency. In addition, selectivity for PDE2 inhibition was relatively poor for **13** and **16** as PDE4 inhibition increased. Interestingly, the dimethylaminopyridine analog **14** displayed excellent PDE2 potency and selectivity versus PDE4, PDE2 IC₅₀ = 1.3 nM; selectivity, 410-fold. Consequently, additional methoxy- and amino- pyridine and pyrimidine analogs, **17–22**, were synthesized. All of these compounds had low nanomolar PDE2 inhibition and greater than 140-fold selectivity over PDE4. Further evaluation of these compounds against a broad PDE panel showed that **22** exhibited excellent selectivity against human recombinant, full length, partially purified PDEs. Compound **22** demonstrated excellent PDE2 selectivity, greater than 1000-fold over PDEs 1B, 3A, 3B, 4A, 4B, 4C, 7A, 7B, 8A, 8B, 9, 10, 11, and between 241-fold to 419-fold selectivity versus PDEs 1A, 4D, 5 and 6.

Table 1
3-Aryl-4-methoxy phenyl analogs in the hydroxypropyl series



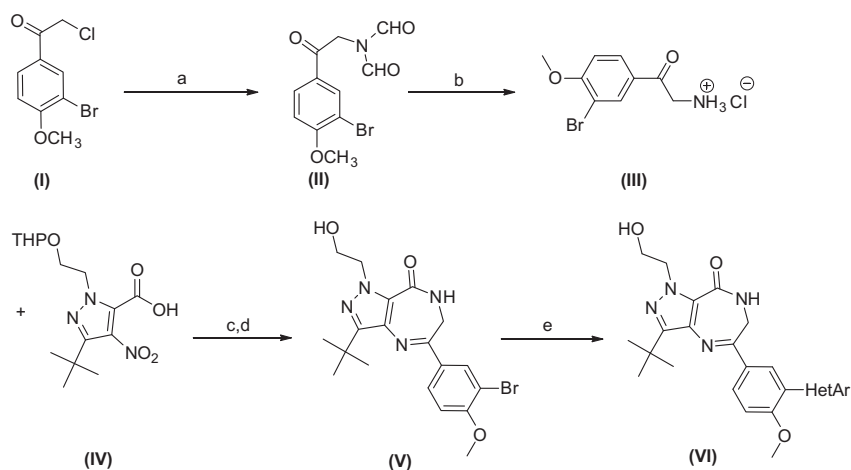
Compound	R=	Catalytic domain PDE2 IC ₅₀ (nM)	Catalytic domain PDE4B IC ₅₀ (nM)	HLM t _{1/2} (min)	Selectivity PDE4/PDE2
2		505	100,000	51	>200
3		483	100,000	120	>200
4		586	8160	48	14
5		156	2070	82	13
6		46	8110	61	176
7		14	100,000	120	>200
8		40	27,000	120	675
9		70	6190	120	88
10		36	6740	120	187
11		18	5660	42	323
12		7	1920	120	263

Each IC₅₀ is the average of at least two independent determinations. Each independent curve consisted of 10 half log dilutions with the 50% inhibition level at approximately the center of the dilution scheme. Each point on the curve was independently determined in duplicate.

Even though all hydroxyethyl compounds had reduced human microsomal stability compared with their hydroxypropyl counterparts, our immediate goal was to establish the unprecedented pharmacology of PDE2 inhibition for OA pain. Thus, we evaluated **22** for bioavailability in rats prior to testing in an efficacy model.

Compounds were evaluated for pharmacokinetic properties in male Sprague–Dawley rats. Two animals were dosed either intravenously (1 mg/kg) or orally (10 mg/kg), and pharmacokinetic parameters were determined. The pyrazolodiazepinone PDE2

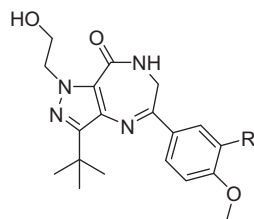
inhibitors **10** and **22** generally provided good oral bioavailability with clearance and half-lives reflecting in vitro microsomal metabolic stability (Table 3). The bioavailability of **10** and **22** would suggest that oral dosing could be readily used in animal efficacy models. However, not all of the compounds studied (data not shown) had such good PK data, therefore, we chose to use subcutaneous (SC) dosing to provide internal consistency within our in vivo studies. Compound **22** has a cLogP = 2.0 and a polar surface area of 124 with a molecular weight of 464 g/mol which are outside the limits of preferred CNS property space, and thus not ex-



Scheme 1. Reagents and conditions: (a) sodium biformylamide, CH₃CN, room temperature, 77%; (b) 6 N aqueous HCl/glacial acetic acid/reflux/60%; (c) EDAC/HOBt/DMF/room temperature, 82%; (d) SnCl₂·H₂O/EtOH/reflux, 66%; (e) (PPh₃)₄Pd, 2M Na₂CO₃, ArB(OH)₂ or HetArB(OH)₂, DMF, 120–150 °C, 30–70%, microwave.

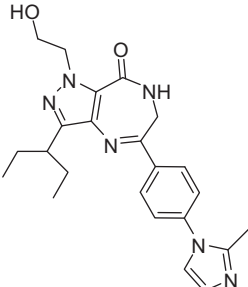
Table 2

3-Aryl-4-methoxy phenyl analogs in the hydroxyethyl series



Compound	R=	Catalytic domain PDE2 IC ₅₀ (nM)	Catalytic domain PDE4B IC ₅₀ (nM)	HLM t _{1/2} (min)	Selectivity PDE4/PDE2
13		6.8	110	59	16
14		1.3	534	74	410
15		3.4	741	43	217
16		9.3	138	36	15
17		1.2	410	33	341
18		1.4	265	39	179
19		1.8	418	57	229
20		2.5	695	36	283
21		2.5	353	18	144
22		3.3	562	34	168

Table 3
Pharmacokinetic parameters for pyrazolodiazepinone PDE-2 inhibitors

Compound	IV $T_{1/2}$ (h)	Cl (mL/min/kg)	V_{dss} (mL/kg)	PO AUC (ng h/mL)	PO T_{max} (h)	%F
	0.53	70	1100	1660	2.25	75
10	0.73	43	2000	1160	0.5	31
22	1.5	27	3020	4530	3.0	78

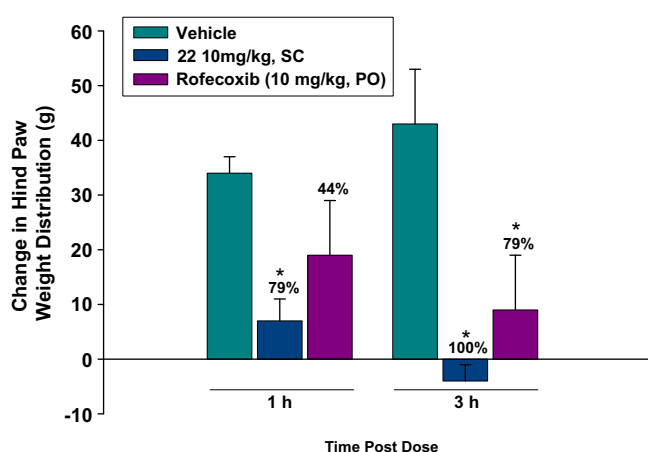


Figure 2. On day 27 post MMT surgery, rats were assessed for change in hind paw weight distribution and distributed into 3 dose groups. The following day (day 28 post surgery) the rats were administered compound or vehicle (sc) and reassessed 1 and 3 h post dose. Data are expressed as mean \pm SEM. Statistically significant differences were determined by one-way ANOVA followed by Dunnett's test. (* P < 0.05 vs vehicle at same time point). N = 6 rats per group.

pected to show good brain penetration.⁷ Additionally, the half-life of **22** in human liver microsomes was only 34 min while in rat liver microsomes it was >60 min. Collectively, these data along with the pharmacokinetic data indicate that **22** should serve as a good tool compound to evaluate the effects of peripheral PDE2 inhibition in rat in vivo models of OA pain. The expected target site of activity is the dorsal root ganglia, which are found outside of the CNS blood brain barrier.

In vivo activity of **22** was evaluated in the rat medial meniscal transection (MMT) model of osteoarthritis pain (Fig. 2).⁸ The MMT model surgically transects the medial meniscus in the right femorotibial joint of the rat. The mechanical disruption of the joint simulates OA-like pain causing the animal to shift weight bearing to the left limb. This shift is measured by placing the animal in a device that assesses weight distribution to each hind limb. Nonsteroidal anti-inflammatory drugs (NSAIDs), cyclooxygenase 2 (COX2) inhibitors, and acetaminophen have been shown to alleviate the imbalance of weight distribution in this model. The time course results of a single, subcutaneous administration of **22** reveal significant inhibition of change in hind paw weight distribution versus vehicle at both the 1 and 3 h post-dose time points and showed sustained activity over the course of the study (Fig. 1). The effect

was greater than that of a single oral dose of the COX-2 inhibitor, rofecoxib. The data suggests that PDE2 inhibition is a novel approach to the treatment of osteoarthritis pain.

Plasma levels of **22** at one hour post dose were 1190 ng/mL (2.5 μ M). Based on the rat plasma free fraction of 3.2%, this plasma level corresponds to a free concentration of 38 ng/mL (80 nM). This is well above the in vitro PDE2 IC_{50} of 3.3 nM and below the IC_{50} of other PDEs suggesting the efficacy is due to PDE2 inhibition. The total brain exposure was 214 ng/mL (475 nM), corresponding to a free brain concentration of 1.9 ng/mL (4.3 nM) based on a rat free brain fraction of 0.9%. Thus, the observed analgesic effect appears to be primarily driven by PDE2 inhibition in the periphery.

Highly potent, highly selective, orally bioavailable, PDE2 inhibitors were discovered through optimization of weak PDE2 activity present in a historic series of PDE4 inhibitors. The PDE2 inhibitors bind orthogonally to PDE2 in a cGMP-like mode when compared to the cAMP-like binding mode observed for this class of inhibitor when bound to PDE4. This binding mode has been confirmed by an inhibitor bound crystal structure in the catalytic domain of PDE2. Replacement of metabolically-labile imidazole biaryls with 3-heterobiaryl-4-methoxyphenyl moieties in the pyrazolodiazepinones has resulted in potent, highly selective, metabolically stable, peripherally restricted, bioavailable PDE2 inhibitors. One of these inhibitors, compound **22**, demonstrated significant in vivo activity 1 and 3 h after a single dose in a rat model of osteoarthritis pain. These results establish selective PDE2 inhibition as a potential new mechanism by which to treat osteoarthritis pain.

References and notes

- Gupta, R.; Kumar, G.; Kumar, R. S. *Methods Find Exp. Clin. Pharmacol.* **2005**, *27*, 101.
- Tegeeder, I.; Schmidtke, A.; Niederberger, E.; Ruth, P.; Geisslinger, G. *Neurosci. Lett.* **2002**, *332*, 146.
- de Vente, J.; Markerink-van Ittersum, M.; Vles, J. S. H. *J. Chem. Neuroanat.* **2006**, *31*, 263.
- Zhang, K. Y. J.; Card, G. L.; Suzuki, Y.; Artis, D. R.; Fong, D.; Gillette, S.; Hsieh, D.; Neiman, J.; West, B. L.; Zhang, C.; Milburn, M. V.; Kim, S.-H.; Schlessinger, J.; Bollag, G. A. *Mol. Cell* **2004**, *15*, 279.
- (a) Suzuki, M.; Iwasaki, T.; Muneji, M.; Okumura, K.; Matsumoto, K. *J. Org. Chem.* **1973**, *38*, 3571; (b) Maeda, S.; Suzuki, M.; Iwasaki, T.; Matsumoto, K.; Iwasawa, Y. *Chem. Pharm. Bull.* **1984**, *32*, 2536.
- Pandit, J.; Forman, M. D.; Fennell, K. F.; Dillman, K. S.; Menniti, F. S. *PNAS* **2009**, *106*, 18225.
- Wager, T. T.; Hou, H.; Verhost, P. R.; Villalobos, A. *ACS Chem. Neurosci.* **2010**, *1*, 435.
- Hook, K. E.; Juneau, P. L.; Connor, J. R.; Kilgore, K. S. *Osteoarthritis Cartilage* **2006**, *14*, 1041.